Modeling of the Transitional Pressure Drop of Fibrous Filter Media Loaded with Oil-coated Particles

Ta-Chih Hsiao[1,*] and Da-Ren Chen[2]

[1]Graduate Institute of Environmental Engineering

National Taiwan University

71 Chou-Shan Rd., Taipei 106, Taiwan

[2]Department of Mechanical and Nuclear Engineering

Virginia Commonwealth University

401 West Main Street, Richmond, VA 23284, USA

Keywords: Fibrous Filter; Aerosol Filtration; Loading Behavior; Oil-coated Particle

Submitted to:

Aerosol and Air Quality Research

* Corresponding author: Ph.: (+886) 2-3366-4401, Fax: (+886) 2-2392-8830.

Ta-Chih (T.C.) Hsiao, Graduate Institute of Environmental Engineering,

National Taiwan University.

Email: tchsiao@ntu.edu.tw

Abstract

The pressure drop of glass-fiber and cellulose filter media when loaded with oil-coated particles was investigated. The focus of this study is to develop a model describing the pressure drop of fibrous filter media under the above particle loading condition. A set of experimental data collected in the previous work was used for this modelling. For the cases loaded with particles having the oil volume percentage less than 50%, a loaded filter was divided into two layers: one layer for collecting all test particles (its layer pressure drop is estimated using the modified Bergman's model) and the other layer remaining clean (its layer pressure drop is calculated using the equation of Davis). The total filter pressure drop is the summation of layer pressure drops. For the cases loaded with particles having oil volume percentage greater than 50%, the experimental data was fitted by a power equation with two parameters (i.e., the exponent, n, and critical volume, V_{cr}). The correlations of the above parameters with the solid-core diameter fraction (X), and the viscosity of coating oils were obtained for glass-fiber and cellulose filter media.

Keywords: Fibrous Filter; Aerosol Filtration; Loading Behavior; Oil-Coated Particle

1. Introduction

Filtration of aerosol particles is a dynamic process. The filter loading process is typically recorded as the filter pressure drop in the function of time (when the size distribution of sampled particles is known) or particle mass/volume collected by filter media of unit area. As particles are trapped in filter media or collected on the media surface, the particle collection efficiency of filter media often continually improves and the pressure drop across the media monotonically increases. While the increase of particle collection efficiency of filtration media is a benefit, the increase in the filter pressure drop is undesirable. It is because the increase of filter pressure drop often results either in the reduction of filtration velocity or the increase in the load of air movers (consequently, reducing the lifetime of air movers).

Various models have been proposed to estimate the time evolution of filter pressure drop when loaded with particles (Endo *et al.* 1998; Kanaoka and Hiragi 1990; Leung and Hung 2008; Saleh and Tafreshi 2014; Thomas *et al.* 1999). The modelling to predict the time evolution of filter pressure drop when continuously loaded with particles, especially in the depth and transitional filtration phases, remains a challenging task. To understand the transitional-loading behavior of filter media, the effect of various factors (e.g., filter medium, physical properties of particles, filtration face velocity, and relative humidity) have been extensively studied. A majority of previous studies have been focused on the loading of filters with only solid particles (Chen *et al.* 2001; Endo *et al.* 1998; Japuntich *et al.* 1994; Joubert *et al.* 2011; Müller *et al.* 2010; Saleh and Vahedi Tafreshi 2015; Song *et al.* 2006; Thomas *et al.* 2001; Veerapaneni and Wiesner 1997) and few on the filtration of liquid particles (Agranovski and Braddock 1998a; b; Liew and Conder 1985; Zhang *et al.* 2017). For liquid particle loading, the droplet migration on fibers in filter media is a very complex process and it is affected by a variety of factors, such as the operational flow condition and the physical property of loaded liquid (liquid viscosity and surface tension) (Chang *et al.* 2016).

In addition to pure solid and liquid particles, particles with a mixed phase (in the form of solid particles coated or mixed with liquids) often existed in the real world. These multi-phased particles are typically called greasy oils. Examples of such greasy particles or oil-coated particles are those emitted from internal combustion engines or generated in vehicle crankcases, and those produced during grinding and milling operations (with metal working fluid) (Hsiao and Chen 2015; Wei *et al.* 2017). Due to their physical property difference, the pressure drop evolution curve of a fibrous filter media loaded with oil-coated particles is very different from that of a medium loaded with either pure solid or pure liquid particles. As a result, the existing pressure drop models for filter media loaded with pure solid or liquid particles cannot be directly applied to describe the filter pressure drop evolution when the loaded with oil-coated particles. One possible method to holistically modeling the loading behavior of a fibrous filter medium loaded with oil-coated particles is to integrate and modify the pressure drop models for filter media loaded with pure liquid and solid particles. The objective of this study is thus to develop a model for predicting the pressure drop evolution of fibrous filter media when loaded with oil-coated particles.

2. Pressure drop of an aerosol filter

Prior to the presentation of our modeling work on the pressure drop of filter media loaded with oily-coated particles, the pressure drop models of clean filter media and loaded filters are briefly reviewed.

2.1 Clean Filter

The basic concept to estimate the clean filter pressure drop is on the force balance. It is assumed that the overall pressure drop results from the summation of drag forces acting on all the fibers in filter media of a unit area. At a low Reynolds number, (i.e., $\rho U d_f/\mu \ll 1$), the drag force on a single fiber can be approximated by the product of the flow velocity, viscosity, and drag coefficient (*f*). The pressure drop of a clean filter, ΔP_0, can then be formulated as

$$\Delta P_0 = F_D \cdot L_f = \mu U f \cdot L_f \quad (1)$$

where F_D is the fiber drag force per unit of fiber length; L_f is the total fiber length per unit area of filter media (which can be derived from the packing density, α_f, and thickness of the filter, Z, when a single fiber diameter, d_f, is given).

$$L_f = \frac{4\alpha_f Z}{\pi d_f^2} \quad (2)$$

The accuracy of the above filter pressure drop modeling is highly dependent on the *f*. Four general expressions of *f* for estimating the pressure drop across a clean filter are summarized in the Table 1.

Table 1. Drag coefficients, *f*, for an individual cylinder fiber.

Expression of *f*	**Reference**
$f = 8\pi \frac{1}{-\ln \alpha_f - \left(\left(1-\alpha_f^2\right)/\left(1+\alpha_f^2\right)\right)}$	Happel (1959)
$f = 8\pi \frac{1}{-\ln \alpha_f - 2\alpha_f - 0.5\alpha_f^2 - 1.5}$	Kuwabara (1959)
$f = 8\pi \frac{1}{-\ln \alpha_f - 1.5}$	Fuchs and Stechkina (1963)

$f = 16\pi\alpha_f^{0.5}\left(1 + 56\alpha_f^3\right)$ for $0.006 < \alpha_f < 0.5$ $f = 16\pi\alpha_f^{0.5}$ for $\alpha_f < 0.006$	Davies (1953)

The expressions for f proposed by Happel (1959), Kuwabara (1959), and Fuchs and Stechkina (1963) were all derived theoretically by solving the flow field in a system of parallel and circular cylinders at a low Reynolds number with different sets of boundary conditions. Happel assumed that the normal velocity and tangential stress at the cylindrical surface are zero (Happel 1959), whereas Kuwabara assumed that the normal velocity and vorticity are zero (Kuwabara 1959). However, experimental results generally indicate that the accuracy of these expressions in predicting filter pressure drops is less favorable than the empirical expression proposed by Davies (1953). The discrepancy between theoretical prediction and experimental measurements is possibly due to the random orientation of fiber cylinders and the flow interference among them in experiments. When the Davies' f expression is chosen and combined with Eqn. (2), the pressure drop of a clean filter can be expressed as

$$\Delta P_0 = \mu U Z \cdot \frac{64\alpha_f^{1.5}\left(1+56\alpha_f^3\right)}{d_f^2} \text{ for } 0.006 < \alpha_f < 0.5, \text{ and} \qquad (3a)$$

$$\Delta P_0 = \mu U Z \cdot \frac{64\alpha_f^{1.5}}{d_f^2} \text{ for } \alpha_f < 0.006 \qquad (3b)$$

The above equations are semi-empirical and do not take into the consideration of fiber size variation in filter medium. A thorough survey by Jackson and James indicated that the prediction begins to deviate from the experimental measurements when the packing density is less than 0.001 (Jackson and James 1986).

2.2 Filter loaded with solid particles

Kanaoka and Hiragi developed an early theoretical model of the pressure drop across a dust-loaded filter, ΔP_l (Kanaoka and Hiragi 1990). They also employed the concept of summing the total drag forces acting on the dust-loaded fibers, F_l, which was evaluated in the manner of Newton's resistance law. The diameter of a dust-loaded fiber (d_{fm}) was chosen as a representative parameter of dendrite structure.

$$\Delta P_l = L_f \int_0^Z F_l \, dz, \text{ and} \tag{4}$$

$$F_l = C_{dm} d_{fm} \cdot \frac{\rho U^2}{2}. \tag{5}$$

The drag coefficient of dust-loaded fibers per unit filtration area (C_{dm}) and the diameter of a dust-loaded fiber (d_{fm}) are two critical parameters in this model. They were correlated with the filtration condition and collection mechanism along with the dimensionless accumulated particle volume, V_{ac}, defined as the loaded particle mass per unit filter volume dividing by particle density and filter packing density. Kanaoka and Hiragi further classified the rate of increase of d_{fm} into three stages: no growth at low V_{ac}, rapid growth at intermediate V_{ac}, and dampened growth at high V_{ac}. This model has been claimed as applicable to predict the pressure drop of a dust-loaded filter under any filtration conditions (Kanaoka and Hiragi 1990). However, the value of d_{fm} and C_{dm} are difficult to be estimated theoretically. They were given by empirically fitting with the accumulated volume of captured particles and cannot be determined without performing experiments.

Instead of evaluating the drag forces of particle dendrites formed by deposited particles, Bergman *et al.* (1978) considered the particle dendrites as newly formed fibers and modified the equation of Davies to include an additional pressure drop due to these newly formed fibers. In addition, to correct the interference between the dendrites and filter fibers, they increased the fiber and dendrite volume fraction by the factors $(L_f + L_p)/L_f$ and $(L_f + L_p)/L_p$ respectively:

$$\Delta P_l = 16\pi\mu U \cdot \left[\left(\alpha_f \cdot \frac{L_f+L_p}{L_f}\right)^{0.5} \cdot L_f + \left(\alpha_p \cdot \frac{L_f+L_p}{L_p}\right)^{0.5} \cdot L_p\right]. \quad (6)$$

where L_p can be evaluated as follows:

$$L_p = \frac{4\alpha_p Z}{\pi d_p^2}. \quad (7)$$

By combining with Eqn. (6), the expression for the pressure drop across a loaded filter can be derived:

$$\Delta P_l = 64\mu U Z \cdot \left(\frac{\alpha_f}{d_f} + \frac{\alpha_p}{d_p}\right) \cdot \left(\frac{\alpha_f}{d_f^2} + \frac{\alpha_p}{d_p^2}\right)^{0.5}. \quad (8)$$

The general criticism of the model of Bergman et al. is on the assumption of a uniform distribution of deposited particles on the filter matrix. Hence, Thomas et al. proposed to divide the entire filter into multiple layers and to evaluated the layers' collection efficiency and pressure drops at every time step based on the information obtained from prior layers (Thomas *et al.* 1999; Thomas *et al.* 2001). Although such a method is ultimately closer to realistic conditions, the calculation is cumbersome and the result can depend on the number of layers, which is arbitrarily determined.

2.3 Filter loaded with liquid particles

For a fibrous filter loaded with liquid particles, only a few models have been established. These models are primarily applicable to filters under steady-state saturation conditions. Liew and Conder performed various tests on filters with mean fiber diameters of 4, 8, 12, and 22 μm and developed an empirical equation to predict the filter pressure drop at the final steady-state stage, ΔP_s (Liew and Conder 1985):

$$\frac{\Delta P_s}{\Delta P_0} = \left[1.09 \cdot \left(\alpha_e \frac{Z}{d_f}\right)^{-0.561} \cdot \left(\frac{U\mu}{\gamma_{LV} \cdot \cos\theta}\right)^{-0.477}\right] \quad (9)$$

where γ_{LV} is the liquid surface tension and θ is the contact angle between a deposited droplet and a fiber.

Raynor and Leith provided another empirical expression for ΔP_s, which is correlated with the steady-state saturation ratio, S_e, and the steady-state packing density, α_e (Raynor and Leith 2000):

$$\ln\left(\frac{\Delta P_s}{\Delta P_0}\right) = \frac{S_e^{0.91\pm0.06}}{\alpha^{0.69\pm0.06}} e^{-1.21\pm0.24}. \quad (10)$$

They also constructed an empirical expression for S_e against the dimensionless numbers (Ca, Bo, Dr) using the commercial statistical software (SAA/STAT):

$$S_e = \frac{\alpha^{0.39\pm0.09}}{\mathrm{Bo}^{[(0.47\pm0.06)+(0.24\pm0.07)\cdot\ln\mathrm{Bo}]} \cdot \mathrm{Ca}^{0.11\pm0.04} \cdot \mathrm{e}^{[(-0.04\pm0.36)+(6.6\pm0.15)\times10^5\cdot\mathrm{Dr}]}} \quad (11)$$

where Bo is the bond number ($\rho g d_f^2/\gamma_{LV} \times 10^5$), Ca is the capillary number ($\mu U/\gamma_{LV} \times 10^5$), and Dr is the nondimensional drainage rate.

Both models are purely empirical and only applicable for certain operational flow ranges. For example, the model of Liew and Conder requires the filter packing density to be larger than 0.02, whereas that of Raynor and Leith is only feasible for a filter thickness of less than 0.88 cm (Liew and Conder 1985; Raynor and Leith 2000). More, these two models only predict the steady-state pressure drop of a liquid-loaded filter.

Frising *et al.* (2005) attempted to establish a pressure drop model for different filtration and loading stages based on the Davies' equation. To imitate the gradual clogging of a filter, they characterized the entire loading process into four stages and divided the filter media into n_p layers with thickness dZ ($i.e., Z/n_p$). In the first stage, the loaded liquid particles are assumed to perfectly coat the filter fibers and form liquid films on or around individual fibers. Therefore, the fiber diameter, d_f, and packing density, α_f, are replaced with the "coated" fiber diameter, $d_{f,w}$, and new packing density ($\alpha_f + \alpha_l$), which includes the loaded droplets.

$$d\Delta p = 64\mu U dZ \cdot \frac{(\alpha_f+\alpha_l)\cdot(\alpha_f+\alpha_l)^{0.5}}{d_{f,w}^2} \cdot \left(1 + 16(\alpha_f + \alpha_l)^{2.5}\right), \text{and} \quad (12)$$

$$d_{f,w} = d_f \cdot \sqrt{\frac{\alpha_f+\alpha_l}{\alpha_f}}. \quad (13)$$

The second stage is defined as the formation of the liquid bridge and liquid film at the fiber intersection, and the diameter of a "coated" fiber remains constant in this stage. Because the air flow is greatly influenced by the presence of liquid bridge and films, the air velocity must be modified. The pressure drop equation for the second stage is given as

$$d\Delta p = 64\mu U dZ \cdot \frac{(\alpha_f + \alpha_{tube}) \cdot (\alpha_f + \alpha_l)^{0.5}}{d_{f,w}^2} \cdot \left(1 + 16(\alpha_f + \alpha_l)^{2.5}\right) \cdot \frac{U}{(1-\alpha_l+\alpha_{tube})} \quad (14)$$

where α_{tube} is the maximal packing density due to the liquid coating the filter fibers. However, α_{tube} cannot be determined either theoretically or experimentally. In the work of Frising *et al.* (2005), the above value was determined empirically to optimize the prediction of the proposed model. In the third stage, the liquid packing density reaches the maximum, and the liquid migration between filter layers begins. The pressure drop is considered constant at this stage. Once the liquid begins to drain out of the filter, the loading process enters the fourth stage, in which

$$d\Delta p = 64\mu U dZ \cdot \frac{(\alpha_f+\alpha_{tube})\cdot(\alpha_f+\alpha_{film})^{0.5}}{d_{f,w}^2} \cdot \left(1+16\left(\alpha_f+\alpha_{film}\right)^{2.5}\right) \cdot \frac{U}{(1-\alpha_l+\alpha_{tube})}, \tag{15}$$

where α_{film} is the maximal liquid packing density and can be estimated by weighing the test filter before and after experiments. Frising et al. reported reasonable agreement between their experimental results and the predictions of their model and stated that the model requires only two parameters - α_{tube} and α_{film} (Frising *et al.* 2005). However, Mullins and Kasper argued that the assumption of perfect liquid coating of filter fibers does not always hold (Mullins and Kasper 2006). For liquids with high surface tension, deposited droplets create liquid beads, rather than forming a film, on the fibers in filter media (Brown 1993).

3. Modeling the pressure drop of filters loaded with oil-coated particles

In our previous experimental study (Hsiao and Chen 2015), the co-solvent method was applied for generating oil-coated particles. A master solution of oil-coated particles was prepared by mixing two parent solutions, coating oil dissolved in 2-propanol and potassium chloride (KCl) dissolved in DI water, using a volume ratio of 1:1. Four coating oils (DEHS, light mineral oil, castor oil, and glycerol) were selected and tested. Accordingly, the loading curve of a filter loaded with oil-coated particles changes from that of a filter loaded with pure solid particles to that of a filter loaded with pure liquid droplets as the thickness of the liquid coating increases. When the liquid volume percentage is less than 50%, the pressure drops of glass-fiber filters and cellulose filters are primarily caused by the solid fraction of the loaded oil-coated particles. More, the loading curve for a low-surface-tension liquid become independent of the liquid's viscosity because the total loaded volume is multiplied by the solid volume percentage. In other words, it was found that all the curves are more closely positioned for both the glass fiber and the cellulose filter media, when the pressure drop evolution curves were re-plotted using the solid core particle volume per unit filter area as the abscissa (Hsiao and Chen 2015). Thus, the model for a filter loaded with oil-coated particles having a liquid volume percentage of less than 50% can be established based on the modified Bergman's method. Because the impaction is the major filtration mechanism in filter media used in our previous testing, the front layer was assumed to collect all particles, and the rear layer was assumed to remain as a clean filter. Thus, the total pressure drop ΔP, of a filter medium is then the linear sum of the pressure drops across these two layers, and Eqn. (3) and Eqn. (8) were used to estimate the values.

$$\Delta P = \Delta P_0{}' + \Delta P_l{}' \tag{16}$$

The thickness of the front layer (Z_{fL}) is the critical parameter for the model's predictions, and was estimated from scanning electron microscopy (SEM) images of the loaded filters. The depths of the front layers used for the glass-fiber filter and cellulose filter were 190 μm and 55 μm, respectively. The other filter characteristics required for the model are listed in Table 2, and α_p was calculated based on the loaded particle volume.

Table 2. Characteristics of the test filter media.

Test Filter Medium	Filter Thickness [mm]	Basic Weight [kg/m^2]	Porosity [--]
Cellulose Filter	0.71	0.136	0.877
Glass-Fiber Filter	0.45	0.112	0.904

As shown in Figure 1, the curves predicted by the modified Bergman's model demonstrated the reasonable agreement with the experimental results for both the glass-fiber filter and cellulose filter up to the pressure drop ratio (defined as the ratio of loaded filter pressure drop to the clean filter pressure drop) of 4. By recalculating the loaded particle volume, the model can be extended to predict the loading behavior for challenged oil-coated particles, which has a coating with a maximum of 50% liquid by volume.

For the loading case with the liquid volume percentage higher than 50%, the transitional behavior is much dynamic and strongly dependent on the liquid's properties (both liquid viscosity and surface tension) as well as the filter medium's characteristics (i.e., either absorptive or non-absorptive). No theoretical/empirical model existed to describe the transitional behavior in the cases. We thus proposed the power-law equation with two parameters, i.e., the exponent, n, and critical volume, V_{cr}, to fit the experimental data. In the proposed equation, n controls the curve growing speed, and V_{cr} controls the curve horizontal scale.

$$\frac{\Delta P}{\Delta P_0} = 1 + \left(\frac{V}{V_{cr}}\right)^n. \quad (17)$$

where ΔP_0 is the initial pressure drop of filter, and V is loaded particle volume per unit filtration area.

A similar approach was employed by Hermans and Bredée (Hermans 1936) and Gonsalves in hydrosol filtration (Gonsalves 1950) and was later applied to aerosol filtration by Emi et al. (Emi *et al.* 1982). Although a satisfactory result was reported by Emi et al. for collection efficiency data, its correlation with pressure drop was not evident. In the present study, however, the loading curves for different oil-coated particles are well fitted by Eqn. (17) for at least up to four times the initial filter pressure drop, shown in Figure 2(a) and (b).

To establish an empirical model for calculating the filter pressure drop when loaded with oil-coated particles, the data reported in Hsiao and Chen (2015) were used. The detail information about different oil-coated particles and the corresponding loading behaviors can be found there. In this study, the data for loading with glycerol-coated particles were not include in this fitting. It is because the surface tension and viscosity of glycerol are very different from those of other coating liquids. More, the effects of surface tension and viscosity on filter pressure drop was difficult to qualitatively differentiate based on the data previously collected. Therefore, the parameters, V_{cr} and n, were only correlated to the viscosity of coating liquids in this work.

To illustrate the fitting result, both V_{cr} and n parameters are plotted as the fraction of solid core in the overall particle diameter (X), instead of the volumetric percentage of coating liquid. The solid-core diameter fractions in oil-coated particles corresponding to 0%, 20%, 50%, 88%, and 100% of liquid-volumetric percentage were 1.0, 0.93, 0.79, 0.49, and 0. As shown in Figures 3 and 4 (for glass-fiber and cellulose filter media, respectively), the values of V_{cr} and n

became invariant when the solid core diameter fraction was greater than 0.79 (for coating liquids with similar surface tension). The effect of liquid viscosity on the fitted V_{cr} and n parameters was negligible. However, below the above critical diameter fraction, the V_{cr} and/or n values started to vary. The observed variation was then correlated with the viscosity of coating liquids.

For the glass-fiber filter, as the solid core diameter fraction approached 0, the value of V_{cr} for different coating liquids approached to the same value (Fig. 3). It implied that the surface tension effect dominated the viscosity effect when loading pure liquid droplets (mist) on a glass-fiber filter medium. Differently, the variation in the power n for different coating liquids was minor for glass-fiber filter media (Fig. 4). The parameter of n was approximately estimated by a polynomial of the third order:

$$n = 1.059 + 1.243X - 1.516X^2 + 0.468X^3 \quad (18)$$

where X is the diameter fraction of solid core in oil-coated particles.

For cellulose filter media, the variation of V_{cr} and n values as a function of solid-core diameter fraction were rather complex (Fig. 5 & 6). It is because not only could coating liquid flow over the fiber surfaces of cellulose media but also be absorbed by fibers (Hsiao and Chen 2015). More, the viscosity of coating liquid completely affected the relative position of the loading curves in a range of solid core diameter fractions. To include the viscosity effect in the filter pressure drop model, Table Curve 3D™ was used to establish the relationship among V_{cr}, n, liquid viscosity, and solid-core diameter fraction of test particles in the cases with cellulose media. Note that the same procedure was also applied to the parameter, V_{cr}, in the cases with glass-fiber filter media.

In the analysis, we normalized the values of V_{cr} for different liquids by the $V_{cr,liq}$ when filter media was loaded with pure liquid particles, and normalized the viscosity of coating liquids, μ_{liq}, by the water viscosity, μ_w. As shown in Figure 7, 8 and 9, all three sets of data can be fitted by a polynomial equation, Eqn. (19). The parameters included in Eqn. (19) are listed in Table 3. In general, the values of V_{cr} and n can be obtained from Eqn. (18) and (19) for glass-fiber and cellulose filter media loaded with particles coated with oil liquids.

By Eqns. (17, 18 and 19), the pressure drop evolution curve of glass-fiber and cellulose filter media can be calculated when loaded with oil-coated particles having more than 50% percentage in liquid (i.e., if the solid -core diameter fraction is less than 0.79):

$$\frac{V_{cr}}{V_{cr,liq}} \text{ or } n = A + B \cdot X + \frac{C}{log(\mu_{liq}/\mu_w)} + D \cdot X^2 + \frac{E}{[log(\mu_{liq}/\mu_w)]^2} + \frac{F \cdot X}{log(\mu_{liq}/\mu_w)} + G \cdot X^3 + \frac{H}{[log(\mu_{liq}/\mu_w)]^3} + \frac{I \cdot X}{[log(\mu_{liq}/\mu_w)]^2} + \frac{J \cdot X^2}{log(\mu_{liq}/\mu_w)}$$

$$for\ 0 < X < 0.79 \qquad (19)$$

where *A, B, C, D, E, F, G, H, I,* and *J* are fitting constants.

Table 3. Fitting constants for different V_{cr} and n.

V_{cr} / Glass Fiber Filter		r^2=0.9976		
A=1.202	*B*=5.492E-1	*C*=-1.638	*D*=1.227	*E*=4.072
F=-6.653	*G*=-4.107	*H*=-3.089	*I*=5.015E-1	*J*=7.760
V_{cr} / Cellulose Filter		r^2=0.9983		

A=1.216	*B*=3.135	*C*=-8.778E-1	*D*=5.269	*E*=2.985E-1
F=-1.508	*G*=-4.042	*H*=7.430E-1	*I*=-1.354	*J*=3.543
n / Cellulose Filter		r^2=0.9906		
A=1.330	*B*=6.455	*C*=2.714	*D*=-8.783	*E*=3.631
F=-1.743E1	*G*=1.259	*H*=-3.309	*I*=-1.480	*J*=1.748E1

4. Conclusion

Filtration of oil-coated particles (i.e., greasy particles) are required in the machining factories and exhaust of fuel combustion sources. For loading with oil-coated particles on filter media, the buildup rate of filter pressure drop (defined as the filter pressure drop increase per unit particle mass/volume loaded) reduces and the transitional point of the loading pressure drop curve moves to the high loaded mass regime as the oil volume percentage of oil-coated particles increases. In this work, we established an empirical model to describe the pressure drop curves (i.e., the filter pressure drop as a function of loaded particle volume per unit filter media area) for filter media loaded with particles coated with oils of various thicknesses.

The model consisted of two parts in response to our experimental observations of distinct loading curve characteristics above and below the liquid volume percentage of 50%. For loading with particles with the liquid volume percentages less than 50%, the Bergman's model for solid-particle loading was modified to predict the filter pressure drop evolution up to four times of the initial filter pressure drop. In this part of the modeling, a loaded filter was assumed to have two layers: one layer to collect all oil-coated particles, and the other one remained as a clean medium. The thickness of the first layer can be measured from SEM images. The total pressure drop of loaded filter media was then assumed to be the summation of layer pressure drops.

For loading with particles having the liquid volume percentages greater than 50%, a power equation with two parameters, i.e., the exponent (n) and critical volume (V_{cr}), was introduced to fit the experimental data. The correlations of the above two parameters with the solid-core diameter fraction and oil viscosity were obtained for a glass-fiber filter and a cellulose filter media. The overall pressure drop of filter media loading with oil-coated particles can be thus estimated. Note that the proposed model (Eqn. 17, 18 and 19) for filter media loaded with oil-coated particles shall be limited to the cases with coating oils of low surface tension (< 35 mN/m). It is because the effect of oil surface tension is not included in the experimental data used to develop the proposed model.

Nomenclature

ρ	：Fluid density
U	：Fluid velocity
$\mathrm{d_f}$	：Fiber diameter
d_{fm}	：Diameter of a dust-loaded fiber
$d_{f,w}$	：Coated fiber diameter
μ	：Fluid viscosity
μ_{liq}	：Viscosity of coating liquids
μ_w	：Water viscosity
γ_{LV}	：Liquid surface tension
f	：Drag coefficient
F_D	：Fiber drag force per unit of fiber length
F_l	：Total drag forces acting on the dust-loaded fibers
L_f	：Total fiber length per unit area of filter media
L_p	：Total fiber length of newly formed dendrite per unit area of filter media
Z	：Thickness of the filter
Z_{fL}	：Thickness of the front(loaded) layer
α_f	：Filter packing density
α_p	：Packing density due to newly formed particle dendrites
α_e	：Packing density at steady-state saturation condition (Raynor and Leith 2000)
α_l	：Packing density due to perfectly coated liquid on filter fibers
α_{tube}	：The maximal value due to the liquid coating in the filter
α_{film}	：Maximal liquid packing density
ΔP	：Total pressure drop
ΔP_0	：Pressure drop of a clean filter
ΔP_l	：Pressure drop across a dust-loaded filter
$\Delta P_0'$	：Pressure drop of a clean filter layer
$\Delta P_l'$	：Pressure drop across a dust-loaded filter layer
ΔP_s	：Filter pressure drop at the final steady-state stage
C_{dm}	：Drag coefficient of dust-loaded fibers per unit filtration area
V_{ac}	：Dimensionless accumulated particle volume
V_{cr}	：Critical volume
$V_{cr,liq}$	：
θ	：Contact angle between a deposited droplet and a fiber
S_e	：Steady-state saturation ratio
Ca	：Capillary number (dimensionless)
Bo	：Bond number (dimensionless)
Dr	：Drainage rate (dimensionless)
X	：Diameter fraction of solid core in oil-coated particles

Acknowledgement

This research was financially supported by National Taiwan University from Excellence Research Program - Core Consortiums (NTUCCP-107L891310) within the framework of the Higher Education Sprout Project by the Ministry of Education (MOE) in Taiwan and partially supported by the Center for Filtration Research at the University of Minnesota. This manuscript was edited by Wallace Academic Editing.

References

Agranovski, I. E. and Braddock, R. D. (1998a). Filtration of liquid aerosols on nonwettable fibrous filters. *AIChE journal* 44:2784-2790.

Agranovski, I. E. and Braddock, R. D. (1998b). Filtration of liquid aerosols on wettable fibrous filters. *AIChE journal* 44:2775-2783.

Bergman, W., Taylor, R., Miller, H., Bierman, A., Hebard, H., Daroza, R., Lum, B. (1978). Enhanced filtration program at LLL. A progress report, California Univ., Livermore (USA). Lawrence Livermore Lab.

Brown, R. C. (1993). Air filtration: an integrated approach to the theory and applications of fibrous filters. Pergamon.

Chang, C., Ji, Z., Zeng, F. (2016). The effect of a drainage layer on filtration performance of coalescing filters. *Separation and Purification Technology* 170:370-376.

Chen, C. C., Chen, W. Y., Huang, S. H., Lin, W. Y., Kuo, Y. M., Jeng, F. T. (2001). Experimental study on the loading characteristics of needlefelt filters with micrometer-sized monodisperse aerosols. *Aerosol Science and Technology* 34:262-273.

Davies, C. (1953). The separation of airborne dust and particles. *Proceedings of the Institution of Mechanical Engineers, Part B: Management and engineering manufacture* 1:185-213.

Emi, H., Wang, C. S., Tien, C. (1982). Transient behavior of aerosol filtration in model filters. *AIChE Journal* 28:397-405.

Endo, Y., Chen, D. R., Pui, D. Y. H. (1998). Effects of particle polydispersity and shape factor during dust cake loading on air filters. *Powder Technology* 98:241-249.

Frising, T., Thomas, D., Bémer, D., Contal, P. (2005). Clogging of fibrous filters by liquid aerosol particles: Experimental and phenomenological modelling study. *Chemical Engineering Science* 60:2751-2762.

Fuchs, N. and Stechkina, I. (1963). A note on the theory of fibrous aerosol filters. *The Annals of Occupational Hygiene* 6:27-30.

Gonsalves, V. (1950). A critical investigation on the viscose filtration process. *Recueil des Travaux Chimiques des Pays-Bas* 69:873-903.

Happel, J. (1959). Viscous flow relative to arrays of cylinders. *AIChE Journal* 5:174-177.

Hermans, P. (1936). Principles of the mathematical treatment of constant-pressure filtration. *J. Soc. Chem. Ind.* 55:1-4.

Hsiao, T.-C. and Chen, D.-R. (2015). Experimental observations of the transition pressure drop characteristics of fibrous filters loaded with oil-coated particles. *Separation and Purification Technology* 149:47-54.

Jackson, G. W. and James, D. F. (1986). The permeability of fibrous porous media. *The Canadian Journal of Chemical Engineering* 64:364-374.

Japuntich, D. A., Stenhouse, J. I. T., Liu, B. Y. H. (1994). Experimental results of solid monodisperse particle clogging of fibrous filters. *Journal of Aerosol Science* 25:385-393.

Joubert, A., Laborde, J. C., Bouilloux, L., Chazelet, S., Thomas, D. (2011). Modelling the pressure drop across HEPA filters during cake filtration in the presence of humidity. *Chemical Engineering Journal* 166:616-623.

Kanaoka, C. and Hiragi, S. (1990). Pressure drop of air filter with dust load. *Journal of Aerosol Science* 21:127133-131137.

Kuwabara, S. (1959). The forces experienced by randomly distributed parallel circular cylinders or spheres in a viscous flow at small Reynolds numbers. *Journal of the Physical Society of Japan* 14:527-532.
Leung, W. W.-F. and Hung, C.-H. (2008). Investigation on pressure drop evolution of fibrous filter operating in aerodynamic slip regime under continuous loading of sub-micron aerosols. *Separation and Purification Technology* 63:691-700.
Liew, T. P. and Conder, J. R. (1985). Fine mist filtration by wet filters—I. Liquid saturation and flow resistance of fibrous filters. *Journal of Aerosol Science* 16:497-509.
Müller, L., Comte, P., Czerwinski, J., Kasper, M., Mayer, A. C., Gehr, P., Burtscher, H., Morin, J.-P., Konstandopoulos, A., Rothen-Rutishauser, B. (2010). New exposure system to evaluate the toxicity of (scooter) exhaust emissions in lung cells in vitro. *Environmental Science and Technology* 44:2632-2638.
Mullins, B. J. and Kasper, G. (2006). Comment on:"Clogging of fibrous filters by liquid aerosol particles: Experimental and phenomenological modelling study" by Frising et al. *Chemical Engineering Science* 61:6223-6227.
Raynor, P. C. and Leith, D. (2000). The influence of accumulated liquid on fibrous filter performance. *Journal of Aerosol Science* 31:19-34.
Saleh, A. and Tafreshi, H. V. (2014). A simple semi-numerical model for designing pleated air filters under dust loading. *Separation and Purification Technology* 137:94-108.
Saleh, A. M. and Vahedi Tafreshi, H. (2015). On the filtration performance of dust-loaded trilobal fibers. *Separation and Purification Technology* 149:295-307.
Song, C. B., Park, H. S., Lee, K. W. (2006). Experimental study of filter clogging with monodisperse PSL particles. *Powder Technology* 163:152-159.
Thomas, D., Contal, P., Renaudin, V., Penicot, P., Leclerc, D., Vendel, J. (1999). Modelling pressure drop in HEPA filters during dynamic filtration. *Journal of Aerosol Science* 30:235-246.
Thomas, D., Penicot, P., Contal, P., Leclerc, D., Vendel, J. (2001). Clogging of fibrous filters by solid aerosol particles Experimental and modelling study. *Chemical Engineering Science* 56:3549-3561.
Veerapaneni, S. and Wiesner, M. R. (1997). Deposit morphology and head loss development in porous media. *Environmental Science & Technology* 31:2738-2744.
Wei, X., Chen, F., Wang, H., Zhou, H., Ji, Z., Lin, T. (2017). Efficient Removal of Aerosol Oil-mists using Superoleophobic Filters. *Journal of Materials Chemistry A*.
Zhang, J., Pan, W., Long, Z., Wang, C., Feng, Z. (2017). Study of the Oil Mist Filtration Performance: Pressure Drop Characteristics and Filter Efficiency Model. *Aerosol and Air Quality Research* 17:1063-1072.

List of Tables

List of Figures

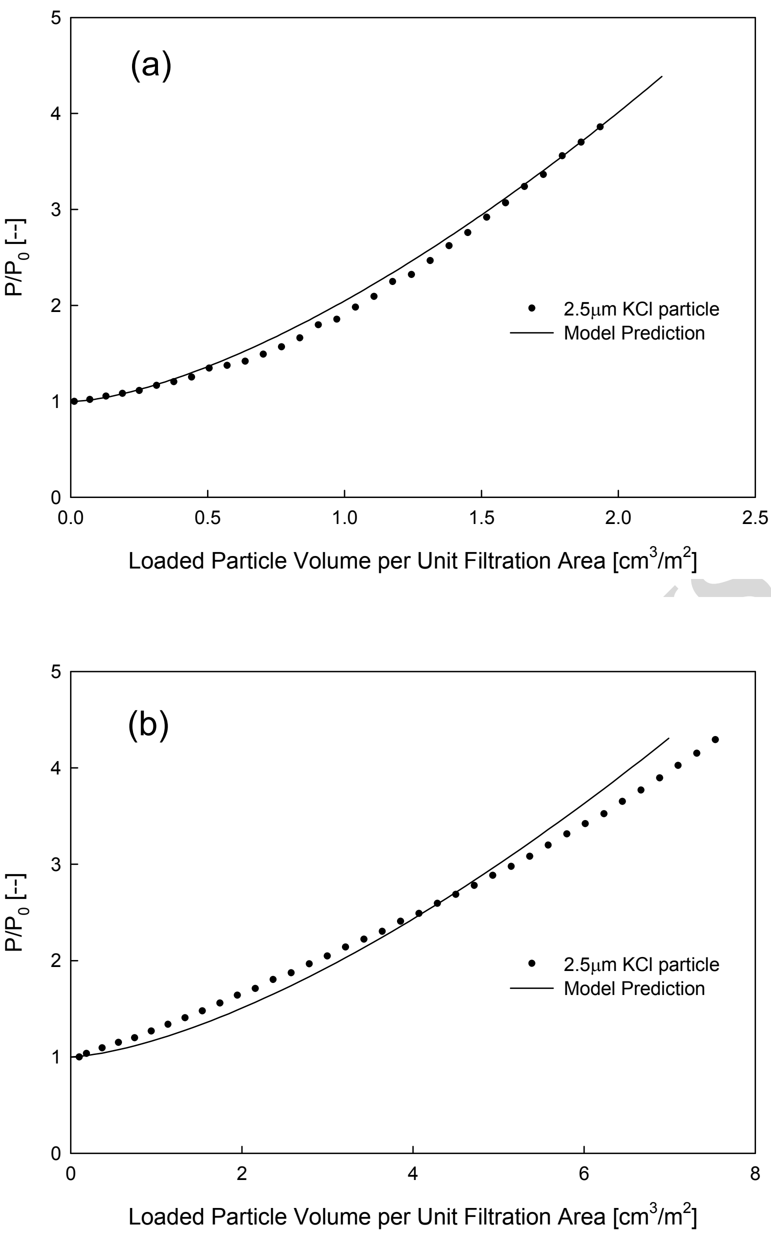

Fig. 1. Experimental data and model prediction for (a) the glass-fiber filter loaded with 2.5-μm solid KCl particles and (b) the cellulose filter loaded with 2.5-μm solid KCl particles.

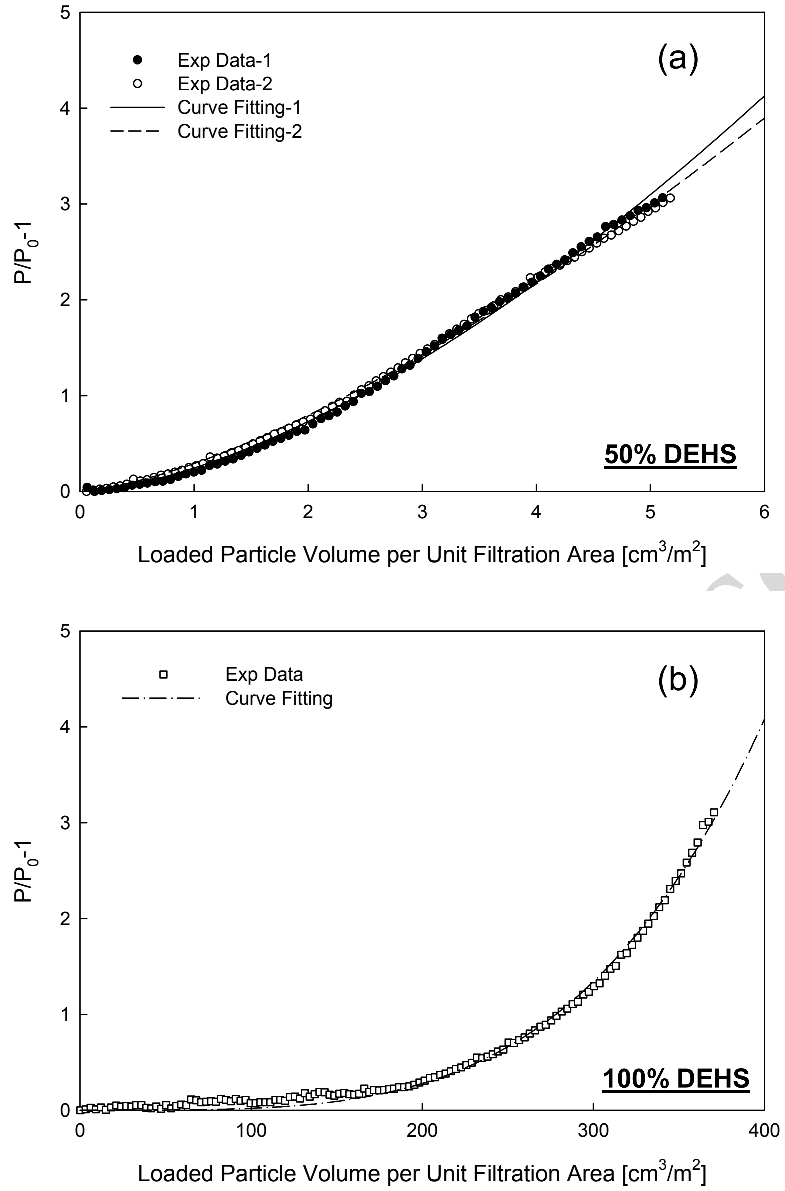

Fig. 2. Experimental data and fitting results for (a) a glass-fiber filter loaded with 2.5-μm 50% DEHS-coated particles and (b) a glass-fiber filter loaded with 2.5-μm 100% DEHS particles.

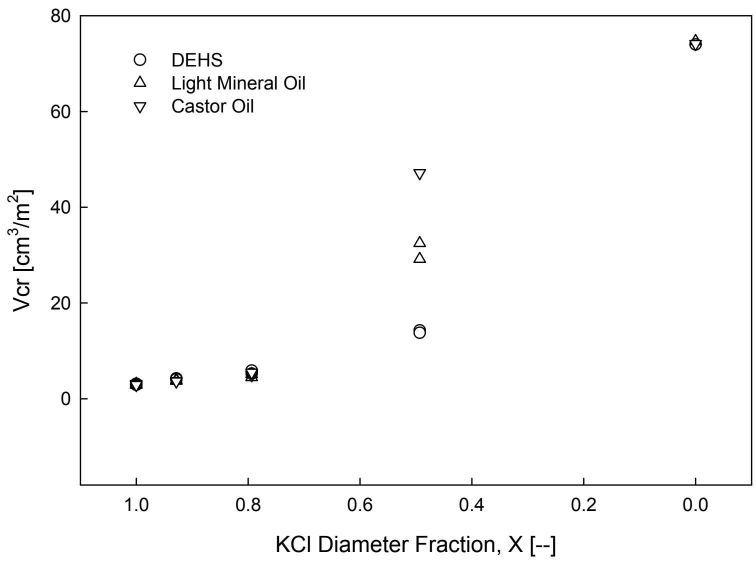

Fig. 3. Critical volume (V_{cr}) of different coating liquids vs. the core diameter fraction for the glass-fiber filter.

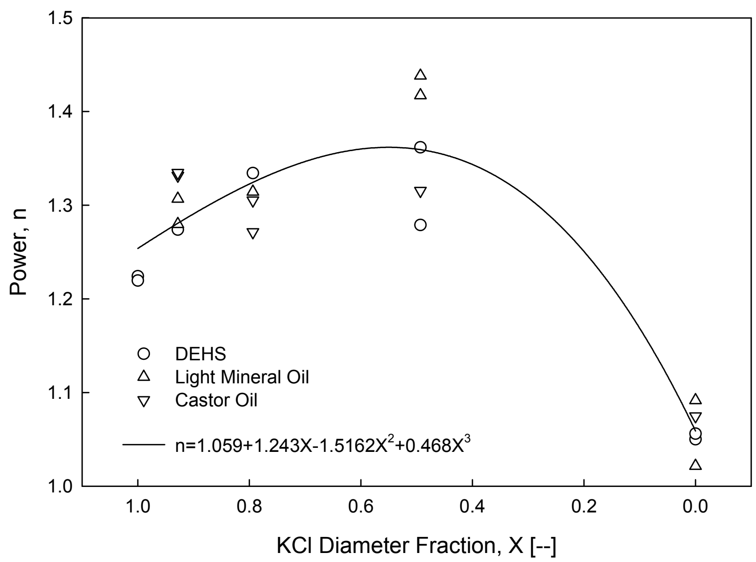

Fig. 4. Exponent (n) of different coating liquids vs. the core diameter fraction for the glass-fiber filter.

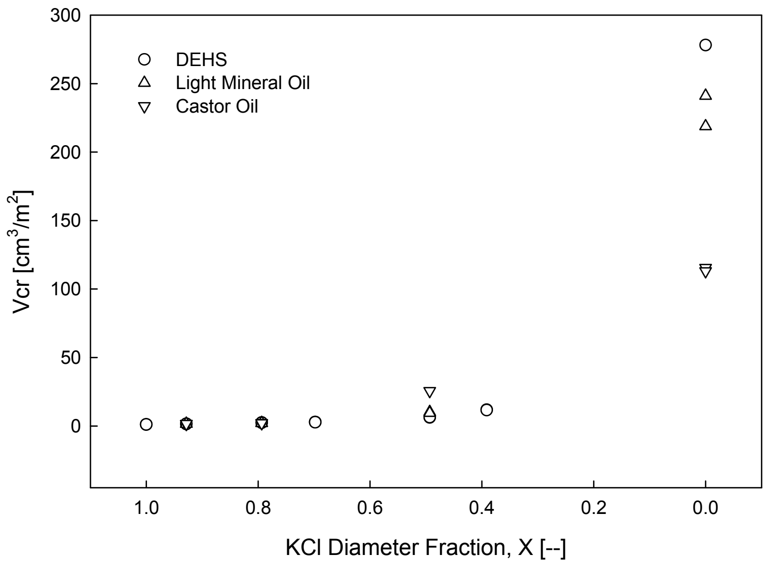

Fig. 5. Critical volume (V_{cr}) of different coating liquids vs. the core diameter fraction for the cellulose filter.

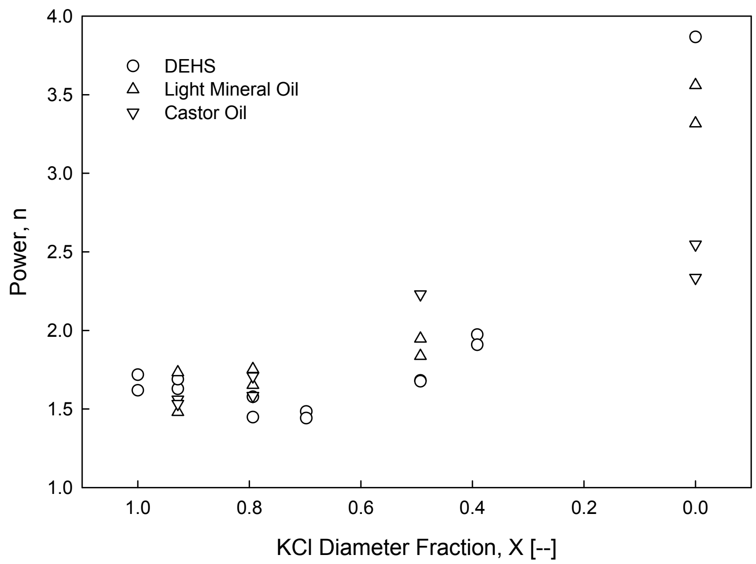

Fig. 6. Exponent (n) of different coating liquids vs. the core diameter fraction for the cellulose filter.

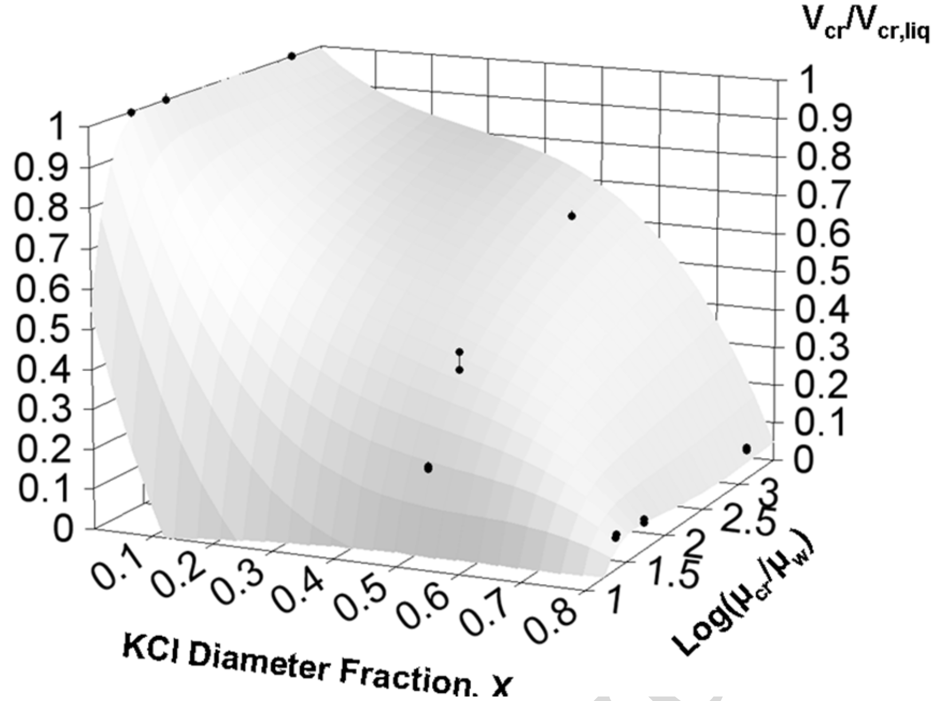

Fig. 7. Fitting result for V_{cr} with the glass-fiber filter.

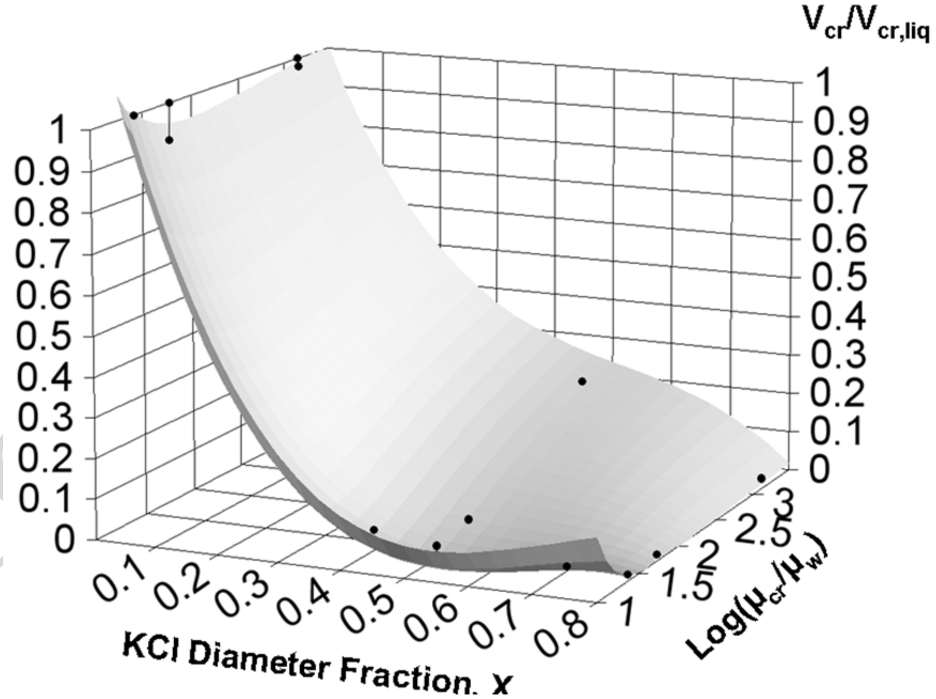

Fig. 8. Fitting result for V_{cr} with the cellulose filter.

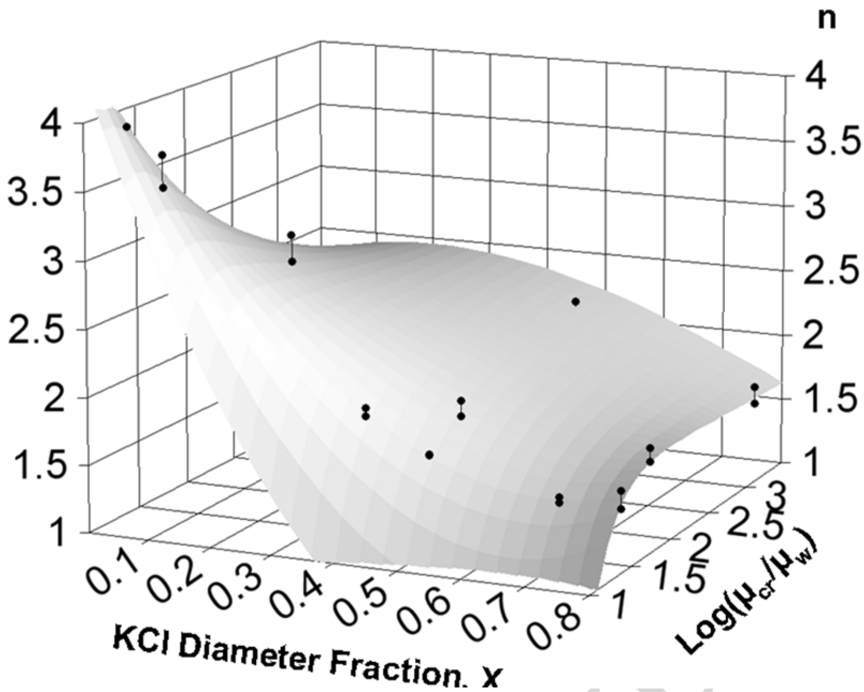

Fig. 9. Fitting result for n with the cellulose filter.